Zoomorphology (2017) 136:1–18
DOI 10.1007/s00435-016-0336-5

ORIGINAL PAPER

Structural analysis of the branchiae and dorsal cirri in *Eurythoe complanata* (Annelida, Amphinomida)

Günter Purschke[1] · Maja Hugenschütt[1] · Lisa Ohlmeyer[1] · Heiko Meyer[1] · Dirk Weihrauch[2]

Received: 6 July 2016 / Revised: 15 November 2016 / Accepted: 19 November 2016 / Published online: 1 December 2016

Abstract In many polychaete species filamentous, pectinate or arborescence branchiae may be present. In species with well-developed parapodia, such as Amphinomidae and Eunicidae, they are often associated with the notopodia. Mostly they arise close to the dorsal cirrus. Whereas the branchiae are regarded as the main site for respiration, the cirri function as segmentally repeated mechanosensory and chemosensory organs. To date, ultrastructural studies exist only for a limited number of polychaete species, especially with respect to the sensory appendages of parapodia. Therefore, the branchiae and dorsal cirri were investigated with CLSM, SEM and TEM in a species of Amphinomidae, *Eurythoe complanata*. These studies revealed that the branchiae are complex organs comprising blood vessels, highly developed circular and longitudinal musculature, neurite bundles, numerous sensory cells and a specialized epidermis and cuticle. The cuticle is thinner than on the trunk, and the blood spaces at the presumed respiratory sites are covered by cell processes, about 130–350 nm thin, thus providing a short diffusion distance. Ventilation is facilitated by a continuous, longitudinal ciliary band. In contrast to the uniform sensory equipment of the branchiae, several types of receptor cells are present on the cirri. Besides two different collar receptors as well as other uniciliated and multiciliated sensory cells, the basal joint of the cirri comprises a few phaosomous photoreceptor cells. These are of the rhabdomeric type, and although ectopic light sensitivity was known for other species, herein such cells are structurally characterized in polychaetes for the first time.

Keywords Gills · Cuticle · Epidermis · Blood vascular system · Musculature · Sensory cells · Photoreceptor cells

Introduction

In many polychaetes elaborate branchiae are present as extensions of the body wall, often closely associated with the parapodia (Rouse and Pleijel 2001). These parapodial branchiae may be single filaments or finger-like extensions of the body wall, tufts of filaments, pectinate or even arborescence (Gardiner 1988). As a rule, they are often heavily ciliated at their edges facilitating rapid fluid exchange on their active surface. Depending on the life-style of their bearers (e.g., tube-dwellers, burrowers or vagile surface forms), branchiae may be regionalized occurring only on a limited number of segments or on many segments. Presence of branchiae is generally family or species specific; however, branchiae have seemingly easily been lost and gained during evolution. For instance, in Eunicida there are family taxa with and without branchiae and even within Eunicidae, species of *Eunice* Cuvier, 1817 possess branchiae, whereas those of *Lysidice* Savigny, 1818 do not have branchiae (George and Hartmann-Schröder 1985). In addition, there seems to be a correlation with body size or more precisely to the surface area/volume ratio: small polychaete species, such as members of Syllidae or interstitial species, generally do not possess specific respiratory organs (Rouse and Pleijel 2001; Westheide 2008).

Ultrastructural studies have been carried out only in a few polychaete species belonging to different families.

✉ Günter Purschke
purschke@biologie.uni-osnabrueck.de

[1] Department of Zoology and Developmental Biology, Fachbereich Biologie, University of Osnabrueck, 49069 Osnabrück, Germany

[2] University of Manitoba, Winnipeg, MB, Canada

These studies revealed a considerable diversity in terms of anatomy and structure of the branchial vessels, especially with respect to the thickness of the epidermal cell barrier and the cuticle between the external medium and the blood, ranging from less than 1 to several micrometers (Storch and Alberti 1978; Storch and Gaill 1986; Jouin and Toulmond 1989; Jouin and Gaill 1990; Rouse and Pleijel 2001; Huusgaard et al. 2012). Many polychaetes that lack branchiae, such as Nereididae, may possess highly vascularized parapodia or parapodial lobes presumably serving as branchiae (Nicoll 1954; Gardiner 1988).

In most annelid taxa, the branchiae are usually associated with the parapodia or, alternatively, they emerge directly from the dorsum between the notopodia and the dorsal midline (Rouse and Pleijel 2001). In the former, they are either directly associated with another kind of parapodial appendage, the dorsal cirrus (Amphinomida and Eunicida), or the notopodial lobe (e.g., Opheliidae), whereas interramal branchiae situated between noto- and neuropodium are unique for Nephtyidae (Rouse and Pleijel 2001). In Amphinomidae, dendritically branched or feather-shaped branchiae may be present from the second or fourth chaetiger and continue on all segments, or they are restricted to a number of anterior segments (Fauchald 1977; George and Hartmann-Schröder 1985).

In general, branchiae are regarded as the site of gas exchange and respiration (Gardiner 1988; Rouse and Pleijel 2001). However, other functions of branchiae have been discussed as well. It was suggested that the highly vascularized parapodia might play a role in excretion and regulation of the internal medium in addition to the metanephridial system (O'Donnell 1997). In fact, recent observations showed that the branchiae in *Eurythoe complanata* (Pallas, 1766) are also involved in ammonia excretion (Thiel et al. 2016). As all marine invertebrates, the polychaete species studied so far are ammonotelic; however, very limited information exists regarding the ammonia excretion mechanism or the actual site of ammonia excretion in other marine annelids. Besides respiration and excretion, branchiae may also serve as sensory structure, which is well known for the dorsal and ventral cirri (Purschke 2005).

Annelids possess a wide range of sensory structures (Verger-Bocquet 1992; Purschke 2005, 2016). These structures may form more or less complex sensory organs, such as eyes and nuchal organs, or represent isolated or clustered sensory cells (Purschke 2016). Among the former photoreceptive structures, eyes and nuchal organs belong to the best investigated sensory structures in annelids (Purschke et al. 2014; Purschke 2016). On the other hand, the sensory appendages have rarely been studied and data for only a few species exist to date (Lawry 1967; Dorsett and Hyde 1969; Boilly-Marer 1972; Schlawny et al. 1991). This might be surprising as for example in *Harmothoe* sp. about 2350 axons were counted in each parapodial nerve, most of which have been regarded to be sensory (Horridge 1963; Bullock 1965). This obviously indicates a great importance of the parapodia and their appendages for the sensory input and for scanning the environment. Moreover, recent studies in transgenic *Platynereis dumerilii* revealed the presence of photoreceptor elements in the ventral nerve cord and in the parapodia (Backfisch et al. 2013), with the latter being reported to constitute a site of the so-called dermal light sense, which is known to exist in many metazoans, but its sensory elements remained largely obscure (Ramirez et al. 2011). With the exception of clitellates (Döring et al. 2013), the structure and distribution of these elements is still almost unknown in annelids.

In the present study, these rare data are supplemented by studying the segmentally arranged branchiae and dorsal cirri in *Eurythoe complanata* (Pallas, 1766) (Amphinomida), belonging to the so-called basal radiation in annelids (Struck et al. 2011, 2015; Weigert et al. 2014). The branchiae in *E. complanata* are equipped with a ciliary band on their narrow edges; cuticle and epidermis on these respiratory appendages are comparatively thin. Each branch is supplied with an ascending and descending blood vessel, elaborated musculature, a nerve and numerous primary receptor cells. Thus, the branchiae exhibit certain characteristics known for polychaetes, such as cilia arranged in bands, a thin cuticle, and blood spaces more or less directly beneath the cuticle. The branchial sensory cells differ from those present in the dorsal cirri, which unexpectedly are also supplied with musculature and a blind-ending blood vessel. Moreover, the dorsal cirri are equipped with simple photoreceptive structures of the phaosomous type in the basal joint. Such segmentally arranged photoreceptive elements are structurally characterized for the first time in annelids, and most likely these parapodial photoreceptive structures are responsible for a dermal light sense.

Materials and methods

Individuals of *Eurythoe complanata* (Pallas, 1766) were obtained from a warm seawater aquarium (salinity 35‰, 20 °C) run at the biology department of the University of Osnabrueck. The original locality of the animals is unknown. To obtain specimens, small quantities of sediment were taken out and treated with $MgCl_2$ solution isosmotic with sea water as described by Westheide and Purschke (1988). Anaesthetized animals were decanted through an 80 µm mesh sieve, revitalized in seawater and then sorted under a dissecting microscope. Prior to fixation intact specimens were anaesthetized again with $MgCl_2$ solution, and fixed immediately after becoming immotile.

For confocal Laser Scanning Microscopy (CLSM) animals were fixed in 4% paraformaldehyde in phosphate-buffered saline (PBS: 140 mM NaCl, 6.5 mM KCl, 2.5 mM Na_2HPO_4, 1.5 mM KH_2PO_4, 12% Sucrose, pH 7.4, 4 °C, 2.5 h). After fixation, specimens were rinsed in PBT (PBS + 0.1% Tween) for 2 h or overnight. Prior to immunolabeling, specimens were dissected and single parapodia or segments were further processed. To increase permeability, specimens were treated with collagenase for 1.5 h (20,000 u/ml Collagenase, 1 mM CaCl, 0.1% Triton X-100, 0.1 M Tris/HCl buffer) followed by PBT + 1% Tween and 1% TritonX-100 for 2 h. After rinsing with PBT, specimens were incubated with PBT containing 0.1% bovine serum albumin (BSA) for 1 h, rinsed in PBT and incubated with the primary antibodies for 2–4 days at 4 °C. The primary antibody was mouse anti-acetylated α-tubulin, (monoclonal, Sigma-Aldrich, Heidelberg, Germany, dilution 1:1000). Following several washes (3× in PBT, 20 min each), the secondary antibodies were applied for 2–3 days at 4 °C (goat anti-mouse, Cy2 conjugated, Dianova, Hamburg, Germany, dilution 1:1000). After being rinsed in PBT overnight, specimens were mounted in Fluoromount (Southern Biotech, Birmingham, USA). For visualizing the musculature, specimens were incubated in fluorescein isothiocyanate-labeled phalloidin for 1 h (100 µg/5 ml EtOH; diluted 1:50 in PBS) and washed and embedded as described above. Specificity of immunoreactivity was controlled by incubating specimens in the same manner, but omitting the primary antibodies. Observations were made with a Zeiss Pascal 5 confocal laser scanning microscope (Zeiss, Jena, Germany). Z-stacks are displayed as maximum projections if not stated otherwise.

For electron microscopy, specimens were fixed in a phosphate-buffered mixture of sucrose, picric acid, glutaraldehyde and paraformaldehyde (SPAFG; see Ermak and Eakin 1976) for 2.5 h at 4 °C and rinsed in phosphate buffer adjusted to the osmolality of sea water (4 °C, 0.075 M, pH 7.2, 12% sucrose, 7 changes, 2 h). Larger specimens were dissected after initial fixation. Post-fixation occurred in 1% OsO_4 for 1 h (phosphate buffered as above) and dehydrated in a graded ethanol series. For SEM, specimens were then critical-point-dried with liquid CO_2 and mounted on aluminum stubs, sputter coated with gold–palladium and examined with a Zeiss Auriga scanning electron microscope. For TEM, after dehydration in ethanol specimens were step wise transferred into the intermedium propylene oxide (EtOH and propylene oxide 1:1, pure propylene oxide). Infiltration with the embedding medium (a mixture of Araldite and PolyBed 812, see Westheide and Purschke 1988) was accomplished by incubating the specimens in a mixture of the embedding medium and propylene oxide (1:3) overnight allowing the intermedium to evaporate. Specimens were then transferred into fresh medium and finally embedded. Polymerization was carried out at 60 °C for 72 h. Ultrathin sections of the parapodia and appendages (70 nm) were made using a diamond knife on a Leica Ultracut E or Leica EM UC 6. Sections were mounted on single slot grids, contrasted with 2% uranyl acetate and 0.5% lead citrate for 30 and 20 min, respectively, in a Nanofilm Surface Analysis Ultrastainer. Sections were examined in Zeiss EM 902A or Zeiss Libra 120 transmission electron microscopes operated at 50, 80 or 120 kV. Micrographs were taken using a 4 K CCD camera, TRS, Moorenweis, Germany. Images were further processed using Image SP©, Adobe Photoshop© and Illustrator©.

Results

Characterization of the branchiae

In *Eurythoe complanata*, the branchiae are situated at the notopodia close to the dorsal cirrus and immediately behind the bundle of notochaetae (Fig. 1a–d). These protective chaetae overtop the branchiae so that they are often hardly visible. The branchiae are dentrically branched and comprise a dorsal and a ventral tuft of flattened branches (Figs. 1b, c, g, 2a–e, 3a). These branches are about 100–200 µm long, 30–50 µm wide and up to 25 µm thick. Each branch is supplied with a band of densely arranged motile cilia at its narrow edges (Figs. 1g–i, 2b, 3a–c, 4a–c). In living animals, the cilia are continuously beating; also their appearance in SEM and CLSM micrographs suggests that they have been beating until fixation occurred (e.g., Figs. 1h, i, 3c). These cilia emerge in small tufts or groups (Fig. 1i), and these groups belong to different cells with each cell bearing 25 cilia on the average (20–39; Fig. 5a). The ciliated cells are arranged in a single row. The cilia are anchored in the cells by a prominent rootlet system. In addition to these motile cilia, there are single short cilia or small tufts of a few short cilia on the flattened sides of the branches (Fig. 1h, i; arrowheads). The distribution of these immotile cilia is somewhat irregular and differs among different branches, and there are more than 10 groups present on each branch (Fig. 1h). These cilia are considerably shorter that those of ciliary bands (2–3.7 vs. 12–18 µm).

Due to the presence of blood vessels, the branchiae are reddish in color in living animals or fresh fixed material (Fig. 2a). The branching pattern of the blood vessels follows those of the branchiae (Fig. 2a). An efferent and an afferent vessel enter the base of each branch and form a hairpin-like loop ending in a long blind-ending needle-like tip (Fig. 4a, c). From the main ascending and descending vessels, irregularly shaped blood spaces extend toward the

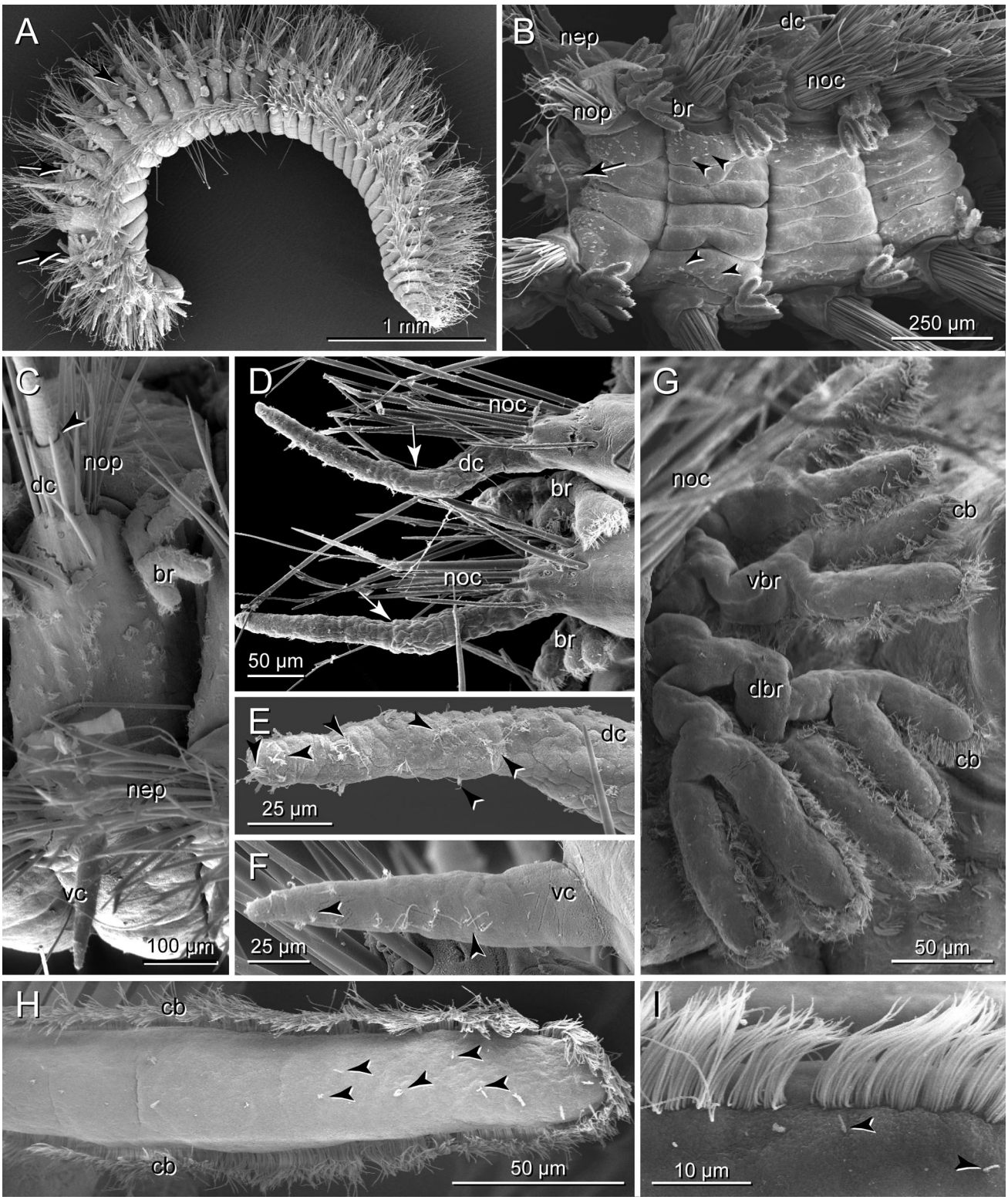
A
1 mm
B
nep
dc
noc
nop
br
250 µm
C
nop
dc
br
nep
vc
100 µm
D
noc
dc
br
noc
br
50 µm
E
dc
25 µm
F
vc
25 µm
G
noc
cb
vbr
dbr
cb
50 µm
H
cb
cb
50 µm
I
10 µm

◀**Fig. 1** External morphology and position of branchiae. SEM images. **a** Entire specimen in *side view*, anterior to the *left*. Note ventrally curved specimen with dorsal cirri and branchiae well protected by notochaetae. **b** Fragmented specimen with four chaetigers regenerating anterior and posterior ends; *arrow* points to developing pro- and peristomium, *arrowheads* point to bundles of sensory cilia on the trunk. Note that branchiae (br) are partly covered by notochaetae (noc). **c** Parapodium in lateral view, noto- and neuropodium (nop, nep) widely separated, dorsal cirrus (dc) anteriorly and laterally surrounded by notochaetae, branchia (br) arising somewhat posterior to parapodium; dorsal cirrus bi-articulated (*arrowhead*). **d** Parapodia in *ventral view* showing arrangement of bi-articulated (*arrows*) dorsal cirri (dc), notochaetae (noc) and branchiae (br). **e** Distal joint of dorsal cirrus with tufts of sensory cilia (*arrowheads*). **f** Ventral cirrus with short indistinct basal joint (*arrow*) and tufts of sensory cilia on the distal joint (*arrowheads*). **g** Enlargement of single branchia branching into dorsal (dbr) and ventral (vbr) group of branchial filaments. **h** Enlargement of single branchial filament with continuous ciliary band (cb) surrounding filament on the narrow edge, several receptor cell cilia marked by *arrowheads*. **i** Enlargement of ciliary band; *arrowheads* point to single sensory cilium. br branchia, ca caruncle, cb ciliary band, dbr dorsal branchia, dc dorsal cirrus, nep neuropodium, noc notochaetae, nop notopodium, vbr ventral branchia, vc ventral cirrus

surface, so that the number of blood spaces visible on a given section varies (Fig. 4a–c). The blood vessels are lined by an extracellular matrix (ECM; 60 nm thick), followed by muscular, coelothelial or epidermal cells (Fig. 5d–f). An endothelium is lacking. The blood vessels form irregularly shaped spaces, which extend toward the periphery (Fig. 5d, e). These blood spaces are covered by thin extensions of the adjacent epidermal cells, which are only 130–350 nm thick in these regions (Fig. 5c–e). They are connected with the main vessels via thin canals extending through the ECM (Fig. 5e).

The blood vessels are accompanied by the highly ordered muscular system comprising longitudinal fibers and thinner circular fibers (Fig. 2b–e). The latter are regularly arranged and comprise only a few individual fibers, whereas the former are thicker and more prominent (Figs. 2e, 5c). These longitudinal fibers taper toward the tips of the branches. Proximally the longitudinal fibers of the individual branches unite (Fig. 2d) and finally join the fibers supplying the dorsal cirrus (Fig. 2c). Thus, in the trunk a single muscle bundle is formed attaching these appendages to the muscular system of the body wall. Distally the muscle fibers terminate somewhat below the tip of the branchiae and are exceeded by the blood vessel (Figs. 2c–e, 4c). For the main part of the branchiae, the blood vessels are centrally bordered by muscle fibers and peripherally by epidermal cells (Figs. 4a–c, 5d–f). The muscle fibers are small in perimeter (approx. 1 by 1 μm) and can be classified as smooth fibers (Fig. 5c).

The branchiae are covered by a collagenous cuticle (1.8 ± 0.3 μm), which is traversed by microvilli (ca. 35 nm in diameter; $n = 18 \pm 4$ μm^{-2}; Figs. 4a–h, 5a, b). Proximally, in the branchiae the microvilli extend above the epicuticle for about 400 nm (Fig. 4g), distally the epicuticle is closer to the microvillar endings (Fig. 4h). Apically, the microvilli branch and form a layer of densely arranged globular tips (60–70 nm wide) giving the surface a pile-shaped appearance in the SEM (Fig. 6e, f). In this region, a prominent glycocalix becomes visible. Beneath the epicuticle (400 nm), several layers of parallel arranged collagen fibers are present in the basal cuticle. The number of layers of collagen fibers and the order of their arrangement decrease toward the tips of the branchiae. Compared to the trunk, the number of microvilli is not significantly increased [14 ± 3.5 (trunk); 18 ± 4 μm^{-2} (branchiae)]. A calculation of the total surface area of the epidermal cells did not reveal higher values for the branchiae compared to the trunk. On the other hand, thickness of the cuticle (5 ± 1 μm) as well as the number of layers of collagen fibers and their highly ordered arrangement differs greatly on the trunk (Fig. 4d–f). In the cuticle of the trunk, a densely arranged monolayer of electron-dense ovoid particles (600 × 600 × 150 nm) can be observed in the epicuticle (Fig. 4d, e), whereas on the branchiae just a few of these structures were observed in the proximal parts only (Fig. 4g) and usually they are absent in the cuticle of the branchiae (Figs. 4a–c, h, 5a, b, d).

The epidermis of the branchiae comprises only a few cell types (Figs. 4c, 5a, b, d). These form a typical epithelium with apical junctional complexes and rest on an ECM. The most common cell type is represented by unciliated supportive cells followed by ciliated cells (see above) and a few gland cells (Fig. 5b). These cells are further accompanied by groups of sensory cells (see below).

Each branchial branch is supplied with a few neurite bundles (Fig. 3a–c). In the median of each branch, a stronger bundle is evident, here called “main branchial nerve” (Fig. 3a, c). This nerve is formed by neurites coming from the short cilia situated on the flattened sides of the branchiae [Figs. 1h, 3c (arrows)]. These cilia belong to uniciliated receptor cells (see below). The number of neurites has not been determined, but given the presence of about 10 sensory buds on each side of the branches and a total of 10 branches comprising a branchia their total number can be estimated to be around 200 neurites. Thus, these neurite bundles increase in diameter toward the bases of the branchiae, unite with the nerve coming from the dorsal cirrus, then with the dorsal parapodial nerve and finally with the main segmental nerve (Fig. 3b, c). In addition, a faint neurite bundle is visible beneath each band of motile cilia (arrowheads in Fig. 3c).

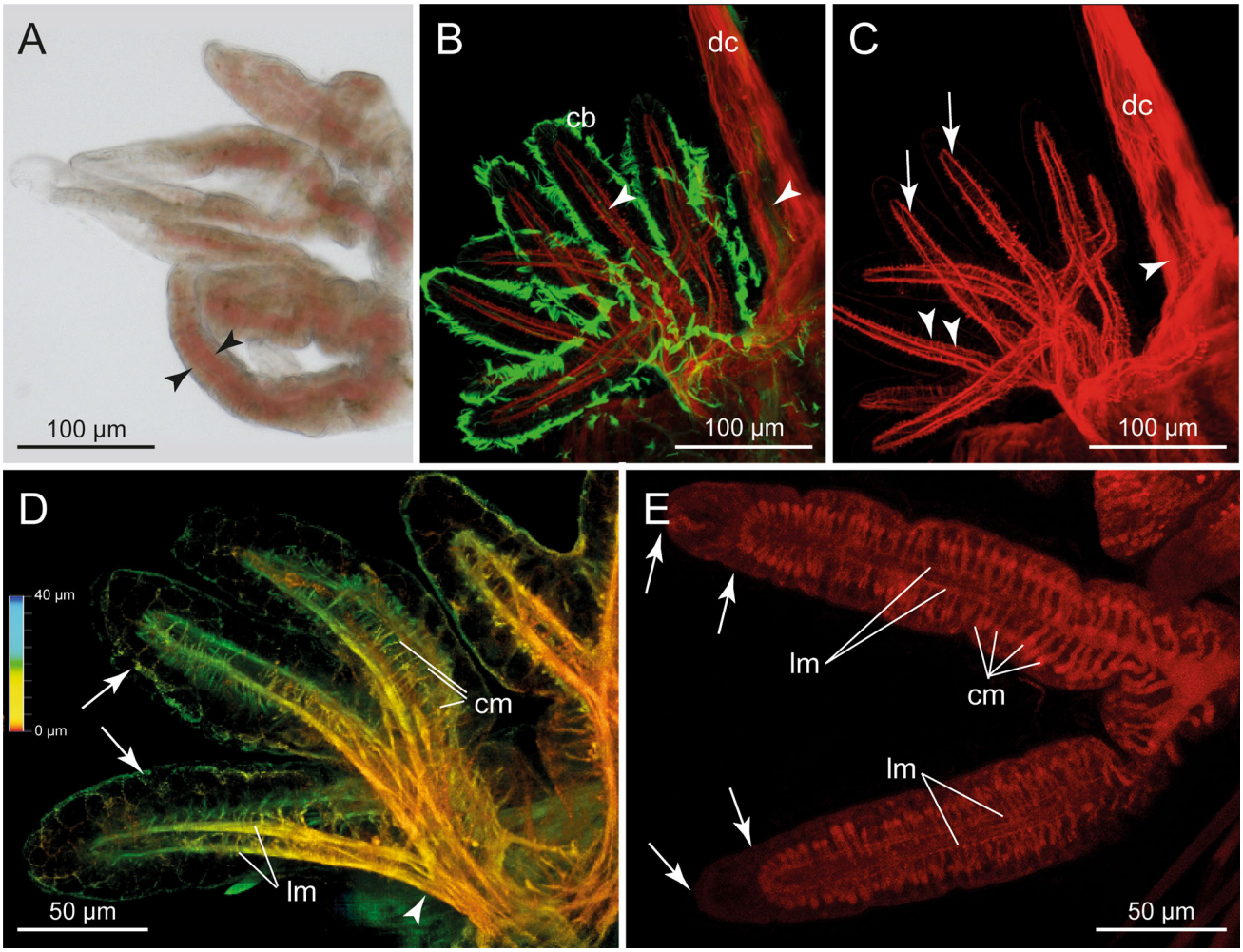

Fig. 2 Musculature of branchiae and dorsal cirrus. A LM, B-E CLSM. **a** Single branchia of fixed specimen, *arrowheads* point to ascending and descending loop of blood vessel. **b** Branchia and dorsal cirrus (dc) staining against acetylated α-tubulin (*green*) and actin (phalloidin, *red*), each branch is supplied with intrinsic musculature and neurite bundles (*arrowheads*); cb ciliary band. **c** Same as **b** showing only phalloidin staining. Each branchia supplied with prominent longitudinal muscle fiber bundles (*arrows*) and smaller circular fibers (*arrowheads*); note strong longitudinal musculature present in dorsal cirrus (dc); circular fibers are only present at its base (*arrowhead*). **d** Musculature of branchiae composed of strong longitudinal (lm) and fine circular fibers (cm) following course of blood vessels; longitudinal fibers show a sharp hairpin-like arrangement; at the base longitudinal fibers unite to a single bundle (*arrowhead*); arrows point to terminal web of actin fibers demarcating position of zonulae adhaerentes. Depth coding image. **e** Two branchial branches with intense stained circular fibers; note that tip of branchiae lack musculature (*between arrows*). cb ciliary band, cm circular muscle fiber, dc dorsal cirrus, lm longitudinal muscle fiber

The dorsal cirrus

The dorsal cirri emerge somewhat behind the protective notochaetae, and their bases are only visible when viewed from behind and ventrally (Fig. 1a–d). The dorsal cirrus is jointed with a basal part comprising almost half of the length (Fig. 1c, d). The dorsal cirri are longer (about 275–300 µm) and finger-shaped compared to the conical ventral cirri, which are about 140–150 µm long in the specimens investigated (Fig. 1c, f). The ventral cirrus possesses an indistinct short basal joint (arrow, Fig. 1f). In the distal joint of both cirri, numerous groups of sensory cilia are visible (Figs. 1e, f, 6a–d).

The dorsal cirrus is supplied with strong musculature forming a continuous bundle reaching from the base and ending somewhat below the distal tip (Figs. 2b, c, 7a, 8a). The muscle bundle is accompanied by a strong neurite bundle located basiepithelially (Figs. 2b, 3a, b, 7a, 8a). Upon reaching the distal joint, the neurite bundle splits up and has a feather-like immunoreactive appearance (Fig. 3a). This splitting pattern is due to the presence of receptor cell somata and their dendritic processes. These somata are located beneath the epidermal supportive cells (Fig. 7a). Between the somata, there are comparatively large intercellular spaces (Fig. 7a), which are absent in the basal joint (Fig. 8a). Basally, the neurite bundle comprises 380–410 neurites of different

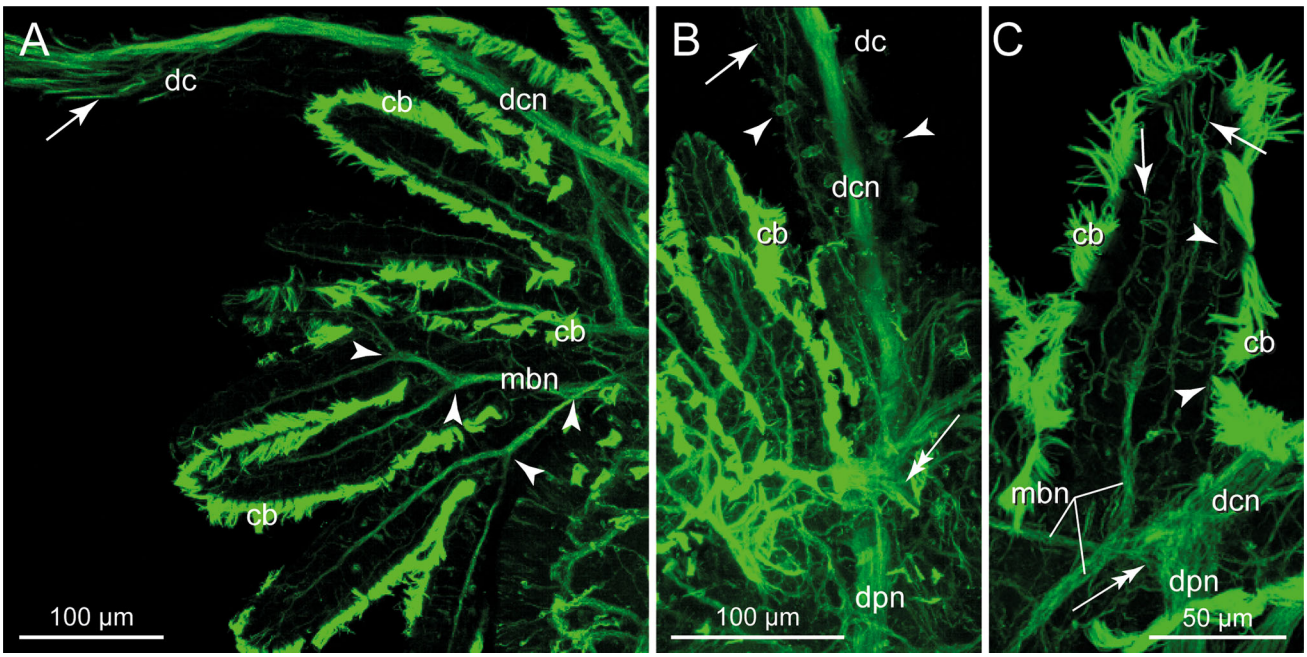

Fig. 3 Innervation of branchiae and dorsal cirrus; CLSM images after staining against acetylated α-tubulin. **a** Entire branchia and proximal part of dorsal cirrus (dc), each branchial lobe is supplied by a strong neurite bundle (mbn) which unite where the branches merge (*arrowheads*); the dorsal cirrus nerve (dcn) splits up into single neurites somewhat above branchia (*arrow*). **b** Dorsal cirrus with strong neurite bundle and a few thinner bundles and receptor cells (*arrow*), note gland cell openings on dorsal cirrus (*arrowheads*), all nerves unite at the base of the cirrus (*double arrow*) and give rise to the dorsal parapodial nerve (dpn). **c** Single branchial lobe and its innervation; several neurite bundles follow the longitudinal axis, *arrows* point to neurites coming from sensory cilia; note faint neurite bundle below ciliary band (*arrowheads*); *double arrow* points to junction of nerves rom branchiae with dorsal cirrus nerve. cb ciliary band, dc dorsal cirrus, dcn dorsal cirrus nerve, dpn dorsal palp nerve, mbn main branchial nerve

diameter ($n = 5$). In addition, a few glial cells are present as well. This nerve finally joins the main segmental nerve.

The proximal part of the dorsal cirrus is entered by a single blind-ending blood vessel, which does not exceed beyond the basal joint of the cirrus. It is bordered by ECM and is completely surrounded by musculature (Fig. 8a). Moreover, there are no branches and blood spaces running toward the surface and cuticle.

The ultrastructure is similar to that of the branchiae, especially with respect to the cuticle, which is likewise comparatively thin, comprising only a few layers of less ordered and thinner collagen fibers than on the trunk epidermis (Fig. 7a). This appearance is unlike in its basal part, where the cuticle is more similar to that of the trunk, including presence of a layer of electron-dense particles in the epicuticle (Fig. 8a). The same applies for the epidermal supportive cells, but ciliated cells with motile cilia are lacking. By contrast, the basal joint is equipped with more gland cells of different types (Fig. 3b). The muscle fibers are clearly obliquely striated.

The receptor cells

The most conspicuous structures of the dorsal cirrus are their receptor cells. Most of them have cilia penetrating the cuticle and usually several cilia form small tufts, as a rule comprising more than 10 cilia (Fig. 1e, 6a–d). Only a few uniciliary receptor cells with cilia not penetrating the cuticle have been observed (not shown). Within the ciliary tufts, mostly 1–3 longer cilia can be distinguished, which are somewhat separated from the rest (Fig. 6b,c). These obviously belong to so-called collar receptors where each cilium is encircled by a ring of microvilli (Fig. 6d). By contrast, the sensory cilia on the branchiae are comparatively short, always equal in length, and usually 3–4 cilia; seldom up to 6 cilia were encountered (Fig. 6e, f). Even more rarely, single cilia were observed on the branchiae as well (Fig. 1i).

The sensory tufts of the cirri always comprise different cell types and most sensory cells are uniciliated (Fig. 7a–i). All sensory cilia exhibit a typical $9 \times 2 + 2$ axoneme. Mostly four different cell types were observed. In each tuft, the separate group comprising long cilia consisted of 1 or 3 cilia, whereas the other group of cilia numbers from 3 to 11 (mean 7.7; $n = 12$, from serial TEM sections). The former belong to two different types of collar receptors. One or two type-1 collar receptor cells were present in every tuft investigated. It is characterized by a circle of 10 strong microvilli extending to the surface (Fig. 7a, b, f). They are somewhat oval in cross section (135 by 80 nm) facing with

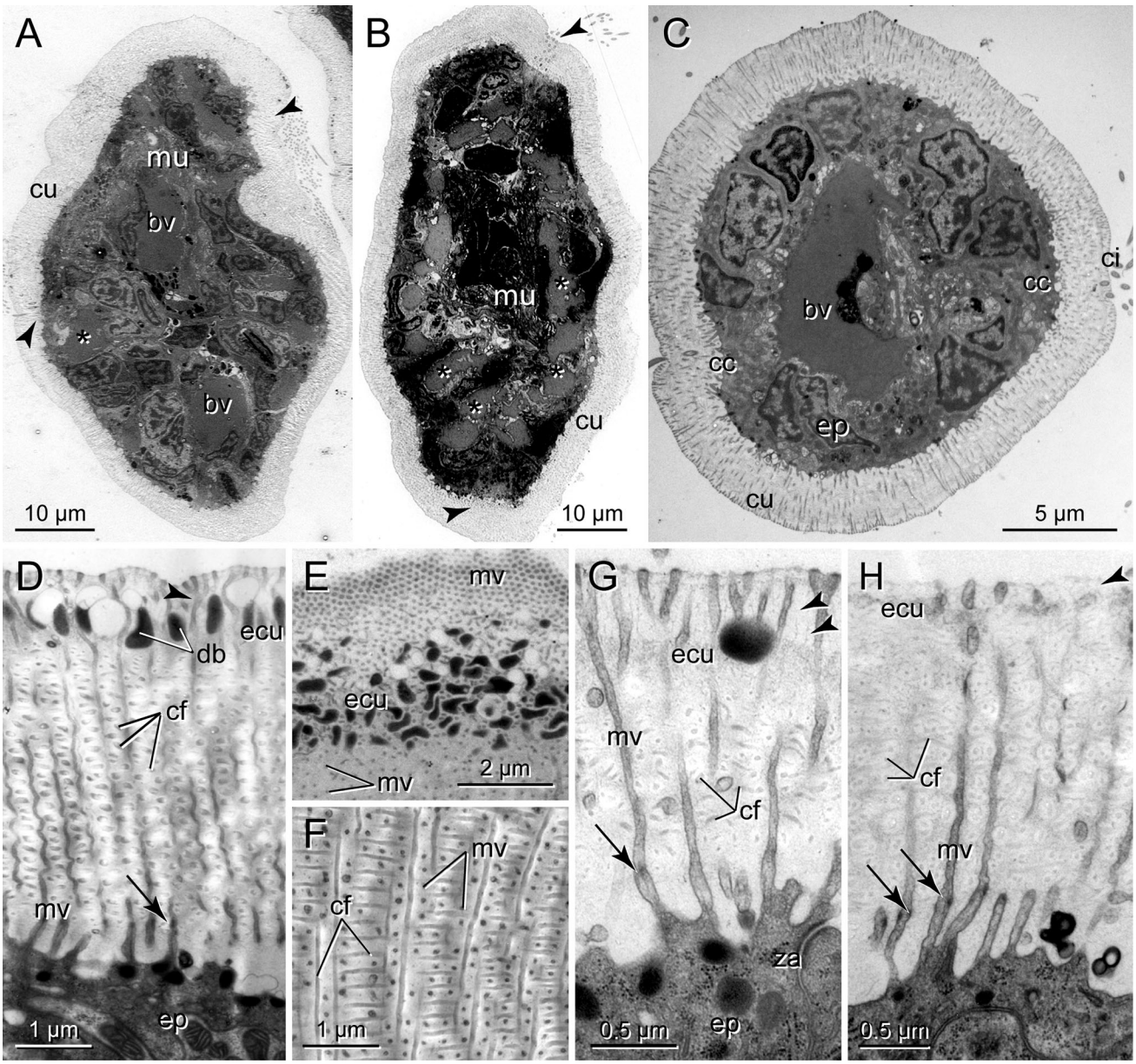

Fig. 4 Ultrastructure of branchiae. **a–c** Low power micrographs showing entire branchial branches in cross section from proximal (**a**) to distal (**c**); *arrowheads* point to ciliary bands, *asterisks* mark blood spaces. **a** Basal region with two main blood vessels (bv). **b** Medial region with central muscle fiber bundle and several blood spaces. **c** Distal part without musculature and single blind-ending blood vessel (bv) **d–f** Cuticle of the trunk. **d** Cross section; note numerous dense bodies (db) in the region of the epicuticle (ec); *arrowhead* points to branching points of microvilli, *arrow* marks apical hemidesmosome. **e** Apical region in tangential section. **f** Middle region in tangential section. **g**, **h** Cuticle of branchiae; *arrowhead* points to glycocalyx, *arrows* to apical hemidesmosomes in basal region of microvilli. **g** Basal region of branchia; note few dense bodies (db) and microvilli extending above epicuticle. **h** Apical part of branchia without dense bodies and epicuticle close to apices of microvilli. bv blood vessel, cc ciliated cell, cf collagen fiber, ci cilium, cu cuticle, db dense body, ecu epicuticle, ep epidermis, mu muscle fiber, mv micovillus, za zonula adhaerens

the smallest side toward the cilium. Due to their high content of thin filaments, they appear comparative electron-dense (Fig. 7b, d, f). Beneath the microvilli, a circular electron-dense cuff, about 0.6 µm in height, is present exhibiting a net-like substructure (Fig. 7c–e). This structure is not attached to the basal body of the cilium (Fig. 7c, e), but the accessory centriole is incorporated into this cuff (Fig. 7d). Basally, rootlet-like structures are attached to the cuff (Fig. 7d, f). The sensory dendrites of the type-1 collar receptors overtop the epithelium for about 1 µm. In this region, the dendritic process gives rise to a few additional microvilli oriented parallel to the epithelial surface (Fig. 7c, f). The dendrites are joined to epidermal cells by typical junctional complexes. In this region, usually an

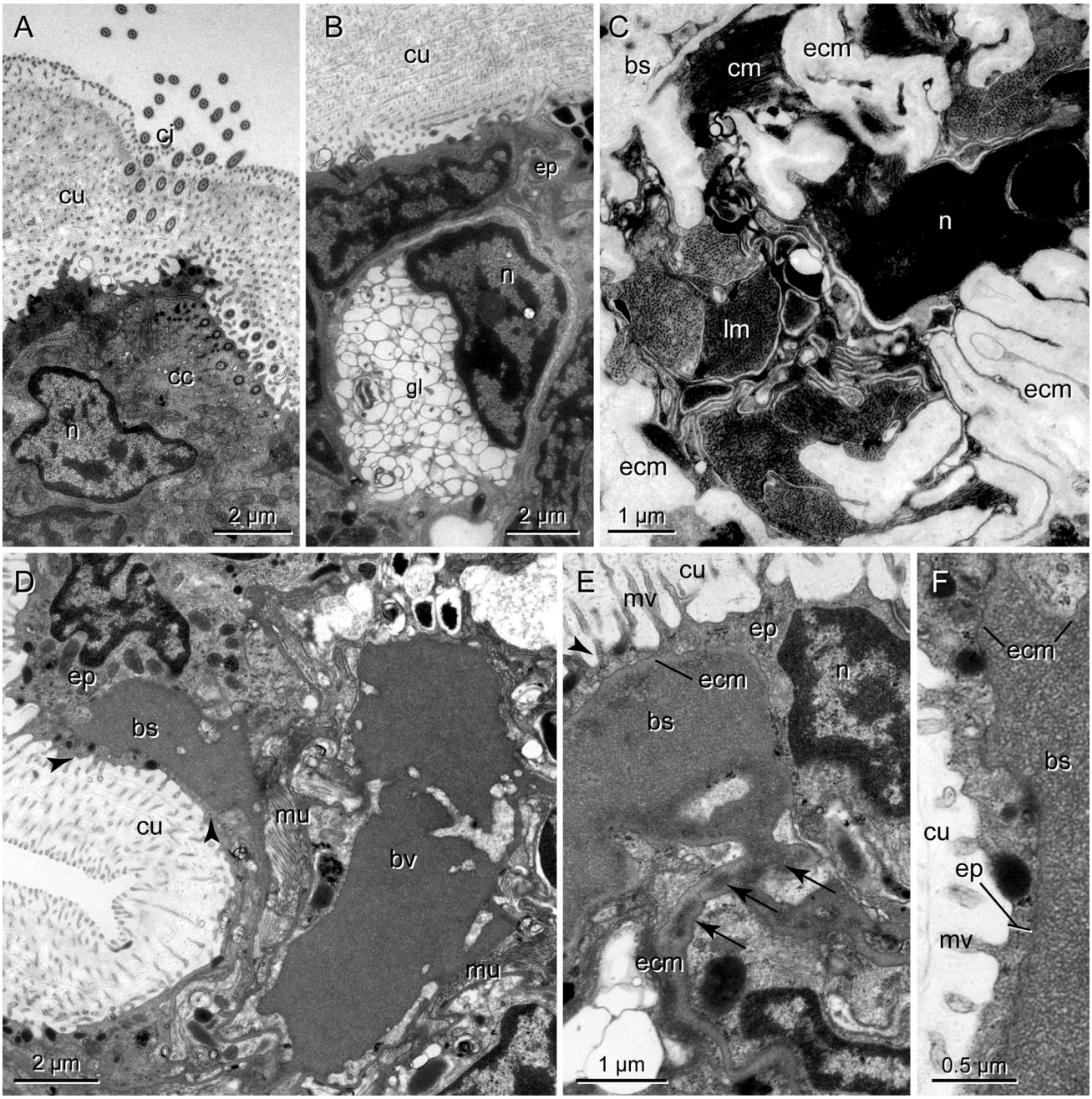

Fig. 5 Ultrastructure of branchiae. **a** Multiciliated epidermal cell (cc) forming ciliary band. **b** Gland cell (gc). **c** Musculature is composed of numerous small longitudinal and circular fibers (lm, cm) surrounded by an ECM (ecm). **d** Blood vessel and intraepidermal blood space (bs); *arrowheads* point to thin epidermal layer separating blood and cuticle. **e** Blood space and connection to deeper regions through spaces in ECM (*arrows*); *arrowhead* points to thin epidermal cover; note continuous ECM surrounding the blood. **f** Enlargement of epidermal cell cover measuring only between 130 and 350 nm. bs blood space, cc ciliated cell, ci cilium, cm circular fiber, cu cuticle, ep epidermis, gl gland cell, lm longitudinal fiber, mu muscle fiber, n nucleus

electron-lucent vesicle measuring about 0.7 µm across is present (Fig. 7d, e). Somewhat below, the dendrites house numerous small electron-dense vesicles (60 nm diameter).

Type-2 collar receptors always represent the third collar receptor cell, if three cells are present in a given tuft (Fig. 7b–e). It possesses only 8 slender microvilli surrounding the cilium which have a diameter of 60 nm. About 600 nm above the cell surface, these microvilli form branches (Fig. 7e, g) so that sometimes more than 8 microvillar profiles are visible (Fig. 7b). Similar to the type-1 cells, these dendritic processes overtop the surrounding epidermal cells (about 0.7 µm high and 1 µm in diameter). As the other collar receptors, they contain numerous electron-dense vesicles. The basal body gives

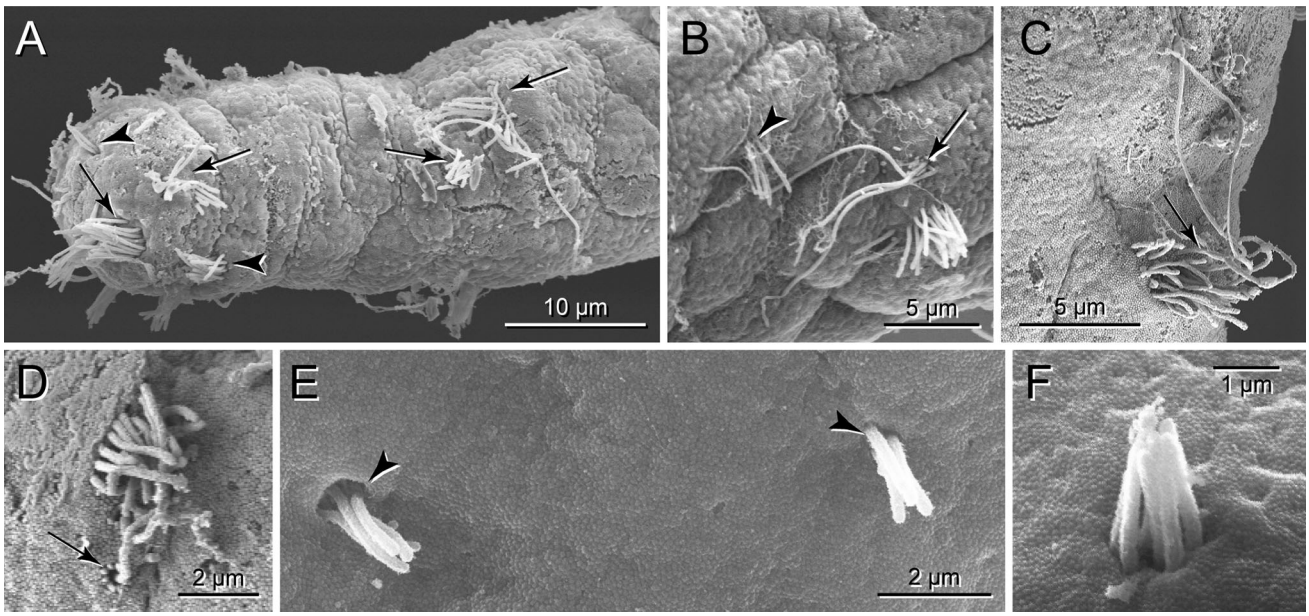

Fig. 6 Sensory cells of dorsal cirrus and branchiae as observed with SEM. **a–d** Dorsal cirrus. **a** Tip of dorsal cirrus with several groups of sensory cilia. *Arrows* point to larger assemblages of cilia with different lengths; *arrowheads* to groups of sensory cilia of equal length. **b–d** Close-ups of different sensory buds. **b** Two different groups of sensory cilia (*arrowhead*, *arrow*); note longer cilia somewhat separated from shorter cilia (*arrow*). **c** Sensory cilia of different length; long cilia are bent toward surface (*arrow*). **d** Longer sensory cilia belong to collar receptors (*arrow*), short cilia emerge close together. **e**, **f** Sensory cilia on branchiae always emerging in groups of 3–4 cilia from common pore in the cuticle (**e**); larger numbers were seldom observed (**f**)

rise to a short and indistinct rootlet; other prominent cytoskeletal elements are lacking (Fig. 7d, g). An accessory centriole is present situated about 1.3–1.5 µm below the apical cell membrane (Fig. 7g).

The group of densely arranged cilia originates from one multiciliated cell giving rise to three cilia and, depending on the total number of cilia in the tuft, to 0–8 additional uniciliated cells. The latter are similar to the type-2 collar receptor cells but lack a microvillar collar (Fig. 7g). They show a diameter of only 0.6 µm and are only slightly higher than the epidermal cells. The multiciliated cells possess constantly three cilia, which arise from the cell apex close together (Fig. 7b, c, h, i). Each basal body gives rise to a distinct rootlet running straight into the cytoplasm for about 1 µm (Fig. 7i).

By contrast, all dendritic processes observed on the branchiae show the same morphology and are different from those present on the cirri. The short cilia in each tuft belong to uniciliated receptor cells (Fig. 7k). Each dendritic process measures about 1 µm in diameter and is part of the epidermis and attached to the epidermal supportive cells by typical junctional complexes. The cilia are about 5–6 µm long and are anchored in the cytoplasm by a basal body. A prominent rootlet is lacking, but microtubules attach to the basal body. As a rule, an accessory centriole is present oriented perpendicular to and somewhat below the

Fig. 7 Receptor cells; TEM. **a** Low power micrograph showing ▶ entire cross section of median part of dorsal cirrus, epidermis (ep) covered by typical cuticle (cu) and followed by layer of somata of receptor cells (so), neurite bundle (ne) close to centrally located group of muscle fibers (mu). *Boxed area* shows position of sensory cilia shown in inset. Note empty spaces between receptor cell somata. *Inset* group of 13 sensory cilia (*arrow*) out of which 3 belong to collar receptors (*arrowheads*). **b**, **c** Cross sections of receptor cell apices. *Boxed* cilia belong to multiciliated receptor cell (type-4), *encircled* cilium to type-2 collar receptor, *arrowheads* point to type-1 collar receptors. **b** At the level of the cuticle type-1 collar receptors are characterized by circle of 10 strong microcvilli, type-2 collar receptors possess 8 branched smaller microvilli, multicilaited cells without microvillar collar. **c** Type-1 cells with apical electron-dense cuff (ec). **d–g** Type-1 and type-2 collar receptors, longitudinal sections. **d** Centriole (ce) associated with electron-dense cuff (ce), inconspicuous rootlet (r) in type-2 receptor, note small dense vesicles (*arrowheads*). **e** Basal body in type-1 receptors cells located above electron-dense cuff; *arrow*: branching microvillus in type-2 collar receptor; *arrowhead*: faint rootlet. **f** Peripheral appearance of microvillar collar, note small rootlet attached to electron-dense cuff (ec). **g** Type-2 collar receptor cell (*left*) and type-3 receptor cells (*right*), both with electron-dense vesicles (*arrowheads*); note deeply positioned centriole in type-3 cells. **h**, **i** Mulitciliated receptor cells with 2 cilia partly sectioned longitudinally. **k** Branchia. Uniciliated receptor cell dendrites (sd) with sensory cilia (sc); basal bodies (bb) without prominent rootlets; arrowhead points to accessory centriole. bb basal body, bv blood vessel, ce accessory centriole, cf collagen fiber, cu cuticle, cu cuticle, so soma of neuron, ec electron-dense cuff, ecm ECM, ep epidermis, mu muscle fiber, mv microvillus, ne neurite bundle, r rootlet, sd sensory dendrite, za zonula adhaerens

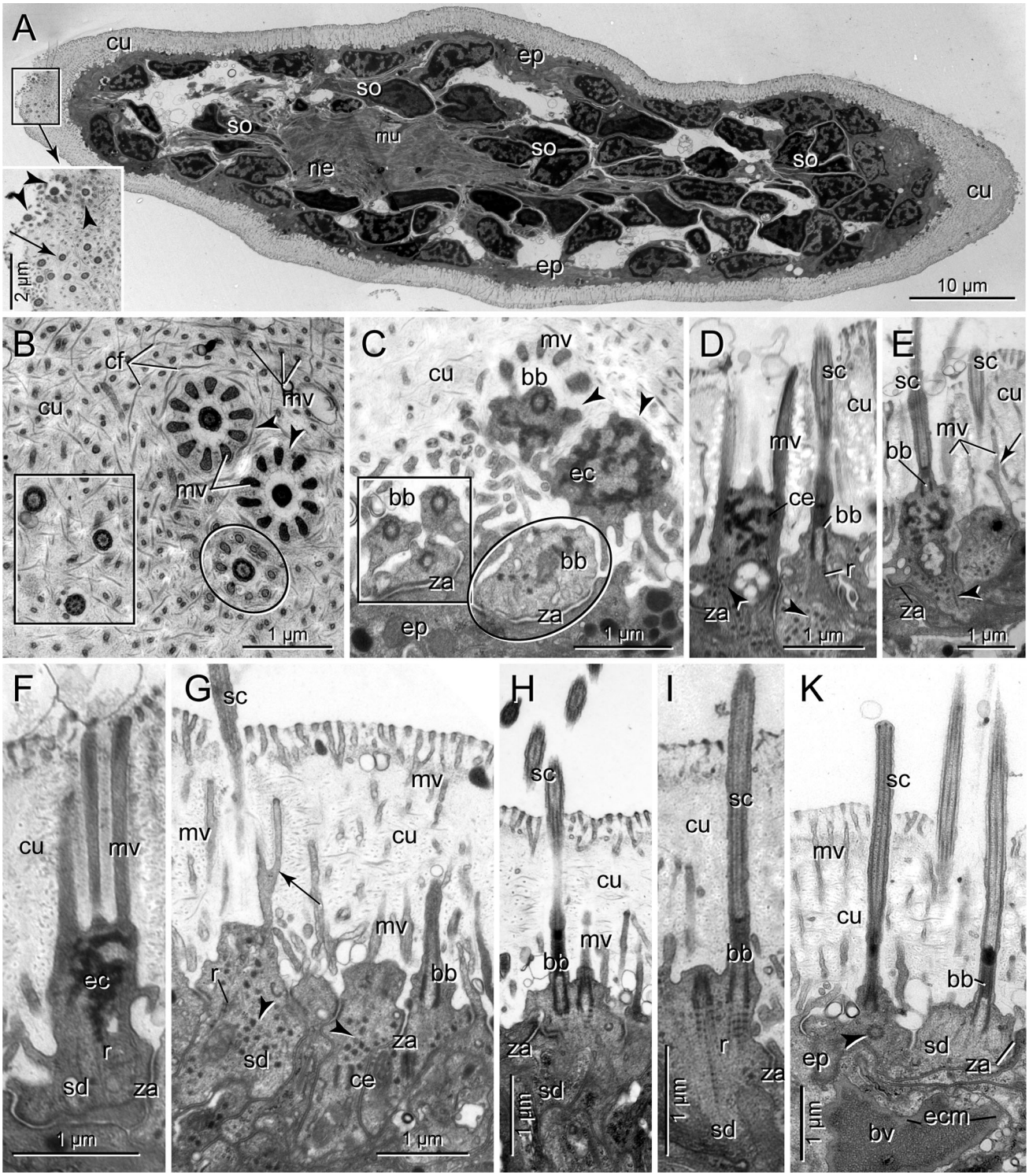
A
cu
ep
so
so
mu
so
so
ne
cu
ep
2 µm
10 µm
B
cf
cu
mv
mv
1 µm
C
mv
cu
bb
ec
bb
bb
za
za
ep
1 µm
D
sc
cu
mv
ce
bb
r
za
1 µm
E
sc
sc
cu
mv
bb
za
1 µm
F
cu
mv
ec
r
sd
za
1 µm
G
sc
mv
mv
cu
mv
r
bb
za
sd
ce
1 µm
H
sc
cu
mv
bb
za
sd
1 µm
I
sc
cu
bb
r
za
1 µm
sd
K
sc
mv
cu
bb
ep
sd
za
1 µm
ecm
by

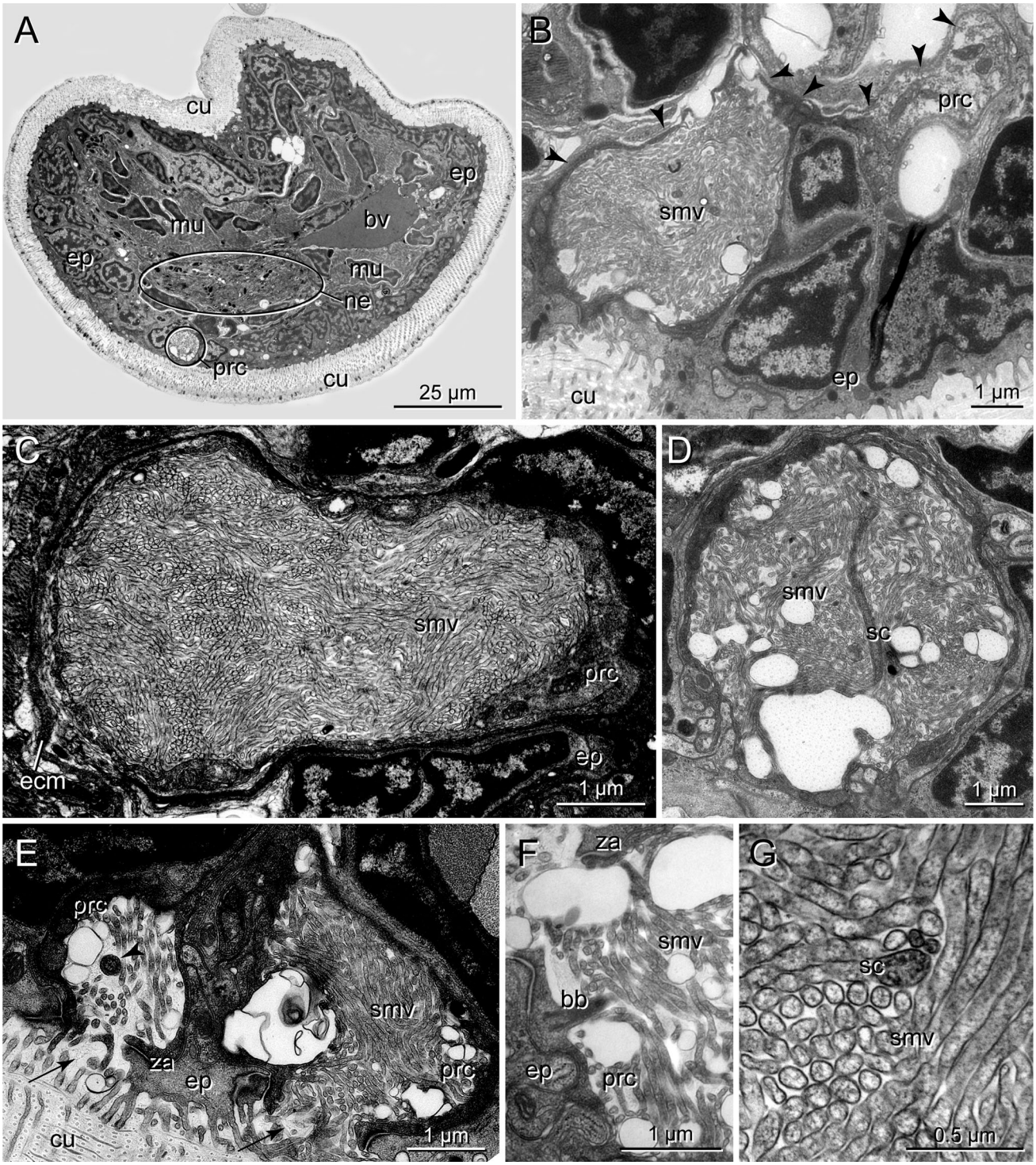

Fig. 8 Photoreceptor-like cell. **a** Cross section of dorsal cirrus, proximal. Blood vessel (bv) surrounded by muscle fibers (mu), photoreceptor (*encircled*) close to central neurite bundle (ne). **b** Cell body of photoreceptor cell (prc) dislocated basally and connected to microvilli-containing part (smv) by thin process (*arrowheads*). **c** Cavity with densely arranged sensory microvilli (smv). **d** Cavity with accessory cilium (sc). **e** 2 closely associated receptor cells with their cavities opening toward the cuticle (*arrows*); *arrowhead* point to cilium. **f** Basal body (bb) of accessory cilium close to opening of cavity. **g** Sensory cilium (sc) and highly ordered microvilli (smv) at higher magnification. bv blood vessel, cu cuticle, ep epidermis, mu muscle fiber, ne neurite bundle, prc photoreceptor cell, sc sensory cilium, smv sensory microvillus

basal body (Fig. 7k, arrowhead). The axonemes exhibit the typical 9 × 2 + 2 pattern of microtubules. In addition to the cilium, each dendritic process bears a few microvilli, which are similar to those of the epidermal supportive cells. All dendritic processes observed were close to an epidermal blood space (Fig. 7k). However, these dendrites are not in direct contact with the vessels but separated by thin epidermal cell processes, 300–400 nm thick.

The photoreceptor cells

The most impressive sensory structures are the simple photoreceptor cells, which were unexpectedly found in each basal joint of all cirri investigated (Fig. 8a–g). At least three of these receptor cells were found in each cirrus. Since there is no shading pigment, they are invisible in the light microscope. The receptor cells are always positioned close to the cirrus nerve (Fig. 8a). As a rule, they occur singly, but sometimes two of them are close together (Fig. 8e). The cells are not associated with supportive cells. They consist of two parts; most obvious is a vacuole-like cavity housing the densely arranged sensory processes (Fig. 8b–d). The cavities are roundish to ovoid and measure up to 5.6 by 6 µm; on the average they are 5 µm across. The part of the receptor cell forming the cavity is rather thin (90–150 nm), while the parts containing mitochondria and other organelles may be up to 0.6–0.8 µm (Fig. 8c, f). The receptor cells are part of the epidermis and form typical junctional complexes with the adjacent epidermal supportive cells, i.e., a zonula adhaerens followed by a septate junction (Fig. 8e, f). The cavity opens to the subcuticular space by a 0.8–1 µm wide opening and thus represents an invagination of the apical cell membrane (Fig. 8e, f). This cavity is filled with numerous microvilli representing the sensory processes (75 by 130 nm), which originate from various places of the apical membrane. For the most part, they are densely arranged and more or less ordered in parallel (Fig. 8c, g). Since the microvilli are twisted, they are always cut in different directions. In the periphery spaces with less or without microvilli are frequently encountered (Fig. 8b, d, e). In addition, each receptor cell bears a cilium, which arises close to the junctional complexes and traverses the entire cavity (Fig. 8d, f). Rootlets were not found (Fig. 8f). The axonemes of the cilia are modified and various patterns of microtubules can be found shortly above the basal body (Fig. 8g). The cell body of the receptor cell is located somewhat deeper in the epidermis and is united via a flat process with the apical part forming the cavity (Fig. 8b). The processes are as flat as the vacuole-forming part and may be a few micrometers long. The cell bodies measure 3.5 by 1.1 µm and contain an electron-dense nucleus. They give rise to an axon, which enters the cirrus nerve close by.

Discussion

Morphology of the branchiae

Besides a general diversity in terms of presence or absence, position and external structure, annelid branchiae exhibit certain common features (e.g., Menendez et al. 1984; Gardiner 1988; Jouin and Gaill 1990; Jouin-Toulmond et al. 1996; Rouse and Pleijel 2001; Jouin-Toulmond and Hourdez 2006; Huusgaard et al. 2012; Shigeno et al. 2014). The appendages usually termed tentacles or palps in vestimentiferan and pogonophoran tube worms (Siboglinidae) also follow these patterns and are likely to represent branchiae as well (Southward et al. 2005). Most polychaete branchiae studied so far are equipped with motile cilia which are either arranged in bands, clusters or tufts effecting continuous and powerful water currents (Gardiner 1988). Very likely, the so-called patch-type of cilia described in *Paralvinella hessleri* represents a similar band of motile cilia responsible for generating water currents (Shigeno et al. 2014). The composition of these bands are seldom described in more detail (see, e.g., Storch and Alberti 1978), but at least in *Terebellides stroemii* these bands are formed by several rows of cells instead of a single row as observed in *E. complanata* (see Jouin-Toulmond and Hourdez 2006). Only *Arenicola marina* appears to be an exception from this general appearance since their branchiae only comprise very few ciliated cells (Jouin and Toulmond 1989). Likewise, epidermis and cuticle are always thinner than in other parts of the body. However, it should be noted that the annelid cuticle is a soft, flexible and not a tight border, which typically is traversed by numerous microvilli (e.g., Welsch et al. 1984; Hausen 2005; Purschke et al. 2014). Their tips usually form a dense cover above the cuticle proper.

Mostly, annelid branchiae are supplied with efferent and afferent vessels, which give rise to some kind of connecting vessel and often blind-ending blood spaces extending deeply into the epidermal cells (Storch and Alberti 1978; Menendez et al. 1984; Jouin and Toulmond 1989). In certain species, afferent and efferent vessel unite to form common long tapering blind-ending distal vessel as observed in *E. complanata* or only blind-ending vessels are present (Nicoll 1954; Clark 1956; Hauenschild and Fischer 1969; Storch and Alberti 1978). Thus, the blood is pumped back into the trunk by the contraction of the branchial musculature. Usually, the distance between the blood spaces and the external medium has been reported to be as short as 1 µm but can be exceeded to 7–10 µm even in comparatively closely related species (Gardiner 1988, 1992; Jouin-Toulmond and Hourdez 2006; Huusgaard et al. 2012). Other studies report thickness of

epidermal cells covering the blood spaces in the same order than observed in the present investigation, which belong to the smallest diffusion distances reported so far (e.g., *Diopatra neopolitana*; see Fig. 8 in Menendez et al. 1984). The thickness of the epidermis outside these extensions of blood lacunae is generally between 7 and 10 µm. As typical for annelids and invertebrates, these vessels represent spaces in the ECM of adjacent epithelia (Fransen 1988; Jouin and Toulmond 1989; Ruppert 1991; Gardiner 1992; Westheide 1997). Whereas in afferent and efferent vessels the ECM is usually lined by myoepithelial or muscle cells, the finer connecting vessels are situated between epidermal and coelothelial cells and the most distal branches only by epidermal cells (Gardiner 1988; Jouin and Toulmond 1989; Jouin and Gaill 1990). In addition, branchiae in certain taxa may also contain coelomic spaces such as observed in *Malacoceros fuliginosus*, *Scalibregma inflatum*, *Arenicola marina* and *Terebellides stroemii* (Storch and Alberti 1978; Jouin and Toulmond 1989; Jouin-Toulmond and Hourdez 2006).

Absence of a well-developed basal labyrinth system in the epithelial cells, usually characteristic of actively transporting cells, led certain authors conclude that branchiae do not have additional functions such as osmoregulation or excretion (Storch and Alberti 1978; see Gardiner 1988). However, Menendez et al. (1984) described a well-developed basal labyrinth system indicative for a transport epithelium in the branchial epithelium of *Diopatra neapolitana*. Moreover, coated pits and coated vesicles have been observed in the branchial epidermis of several species (Menendez et al. 1984; Jouin and Toulmond 1989). Since a basal labyrinth system has not been observed in other annelids, physiological studies are needed to clarify whether they have additional functions besides gas exchange in annelids such as ammonia excretion as has been shown in the species of the present study, *E. complanata* (Thiel et al. 2016). Also the degree to which branchiae contribute to respiratory requirements has been controversially discussed, which was based on the minimal diffusion distances observed in different species (Gardiner 1988). However, it should be noted that in several species investigated no measurements have been provided and certain micrographs indicate epithelium thicknesses of less than 1 µm; e.g., in *Diopatra neapolitana* (see Menendez et al. 1984) or in *Alvinella pompejana* (see Jouin and Gaill 1990). These values are probably in the same range as observed here for *E. complanata*.

Thus far, innervation patterns of branchiae have not been studied in detail except for mentioning presence of sensory cells and neurite bundles (Storch and Alberti 1978; Storch and Gaill 1986; Jouin and Toulmond 1989; Huusgaard et al. 2012) and a more detailed analysis in *Paralvinella hessleri* (see Shigeno et al. 2014). In *E. complanata*, the main branchial nerve very likely mainly comprises the neurites of the receptor cells and is as such an afferent nerve. This is further supported by the fact that these branchial nerves unite with the dorsal cirrus nerve which as a whole represents a sensory organ. Moreover, these fibers join the main segmental nerve entering the ventral nerve cord. Thereby, the small nerves lying beneath the ciliary bands may be efferent nerves modulating the ciliary activity as well as innervating the muscle fibers.

The receptor cells

Annelids respond to a wide range of sensory stimuli and possess a variety of sensory structures which either occur in the form a single receptor cells, groups of receptor cells or more or less complex sensory organs (Bullock 1965; Storch and Schlötzer-Schrehardt 1988; Verger-Bocquet 1992; Purschke 2005, 2016). Receptor cells occurring on the appendages of the head or the trunk have only seldom been studied (Dorsett and Hyde 1969; Boilly-Marer 1972; Schlawny et al. 1991; Purschke 1993; Shigeno et al. 2014).

Generally, these receptor cells can be classified by the number of cilia present and whether or not these cilia penetrate the cuticle as (1) multiciliated penetrative receptor cells, (2) multiciliated non-penetrative receptor cells, (3) uniciliated penetrative receptor cells including collar receptors and (4) uniciliated non-penetrative receptor cells (Purschke 2016). With the exception of multiciliated non-penetrative receptor cells, all cell types were found in *E. complanata*. Due to their external or internal morphology such receptor cells may be subdivided into several subtypes (e.g., Purschke and Hausen 2007; Shigeno et al. 2014). In contrast to the observations in species of Nereididae and Polynoidae (see Lawry 1967; Dorsett and Hyde 1969; Boilly-Marer 1972), a greater morphological diversity of receptor cell types was found on the parapodial cirri in *E. complanata*. This diversity may be indicative for different modalities or different sensitivity of the receptor cells although their function remains speculative. Also in the head appendages of *Ophryotrocha* and Protodrilida species, several different receptor cells types have been described (Schlawny et al. 1991; Purschke 1993) and it can be assumed that this is a general pattern for many annelids (Purschke 2005). Data on the number of receptor cells on parapodial appendages are scarce, but the numbers found in the present investigation appear to be lower than in the other species investigated: Horridge (1963) counted about 2350 neurites in the parapodial nerve and Lawry (1967) found about 900 fibers in the base of the ventral cirrus in *Harmothoe* sp. A 1:1 relationship of receptor cells and efferent axons in the parapodial and segmental nerves is generally assumed so that in *Harmothoe* sp. the number of receptor cells in the parapodia is estimated to be around

2000. Provided a lower number of receptor cells in the ventral cirri, the number of sensory cells in *E. complanata* is only about one-third of the numbers as in *Harmothoe* sp., but this still strikingly shows the great importance of these appendages for sensing the environment.

Uniciliated receptor cells are widespread among annelids, but their modality can hardly be inferred from their structure alone (e.g., Purschke 2005, 2016). Usually, they are characterized by a thin dendritic process measuring about 1 µm or less across and a soma situated somewhat below the level of the epidermal supportive cells. The dendritic processes usually extend above the level of the adjacent epithelial cells. Many of these receptor cells possess a circle of microvilli surrounding the cilium and, therefore, they are called collar receptors. In annelids, these mostly possess a circle of ten comparatively large microvilli with a dense and well-developed system of actin filaments such as observed here for the type-1 receptor cells. Such receptor cells are typical elements of the lateral organs present in many species of Sedentaria and Eunicida (Purschke and Hausen 2007). Whereas so far a circle of ten microvilli has mostly been determined in annelid collar receptor cells, a circle of eight branched microvilli is rarely encountered. To our knowledge, it is reported here for the first time in annelids. With respect to the additional structures present in the sensory dendrites, a comparable diversity has been observed across annelids. Thereby, electron-dense cuffs present at the microvillar bases have been found repeatedly in different annelid receptor cells, but due to their scattered occurrence a systematic significance of this feature cannot be inferred (Jouin et al. 1985; Schlawny et al. 1991; Purschke 1993, 2005). Likewise, a high diversity of collar receptor cells has been described in other invertebrates such as in acoels (Todt and Tyler 2007). This led the authors casting doubts on a general homology assumption of collar receptor cells among metazoans in contrast to the view of many other authors (see e.g., Purschke 2005; Schmidt-Rhaesa 2007).

In contrast to the sensory elements present on the dorsal cirri, it appears remarkable that the receptor cells observed in *E. complanata* are morphologically uniform. Due to the absence of a microvillar collar, they cannot be classified as collar receptor although being uniciliated. These receptor cells differ from those described on the branchiae in *Alvinella pompejana* which are multiciliated (Storch and Gaill 1986). However, in the few data available only one receptor cell type is figured or mentioned. Also in the hydrothermal vent annelid *Paralvinella hessleri* only one type of sensory cells has been described by Shigeno et al. (2014). In *E. complanata*, their probable function may be measurement of chemicals such as oxygen, carbon dioxide, ammonia. Alternatively, these cells may be mechanoreceptive responsible for measuring the water currents running along the surface of the branchiae. Although the functional significance is unclear, it appears noteworthy to mention that the dendritic processes usually terminate close to a subepidermal blood space in *E. complanata*. We could not observe a direct contact of these receptor cells with the blood which might be indicative for a certain kind of measurement such as oxygen content. Interestingly, preliminary observations on the branchiae in *Scoloplos armiger* (OF Müller, 1776) likewise showed a similar arrangement of blood spaces and receptor cell terminals (Purschke et al. unpubl. obs.).

The photoreceptor elements

Most annelid species possess some kind of photoreceptor cell or light sensitive organ (Rouse and Pleijel 2001). In annelids, three different types of photoreceptor cells (PRCs) are generally distinguished: rhabdomeric PRCs, ciliary PRCs and phaosomous PRCs (see Purschke et al. 2006; Purschke 2016). The former occur together with supportive cells, and the sensitive processes are housed in an extracellular cavity formed by the apical surfaces of these cells. In the phaosomous PRC type, the sensitive processes (either cilia or microvilli) are found in a seemingly intracellular vacuole which, however, was ontogenetically formed by an invagination of the apical cell membrane. In both cases, these cavities may communicate with the exterior or the subcuticular space, as found in the PRCs of *E. complanata* (Purschke 2003; Suschenko and Purschke 2009; Purschke and Nowak 2015).

Whereas photoreception is generally accepted if these receptor cells are associated with shading pigment, this is regarded as unclear if such cells are not associated with shading pigment. In these cases, photoreception was inferred form structural characteristics of photoreceptor cells alone. Most important among these characters is a great expanse of the apical cell membrane providing sufficient space for the photosensitive pigments, the opsins (Eakin and Hermans 1988; Purschke et al. 2006). However, in recent times it could be shown that at least in certain species such cells in fact express opsins, providing strong evidence for photoreception in unpigmented PRCs as well (Arendt et al. 2004, 2009; Backfisch et al. 2013; Döring et al. 2013; Randel et al. 2013). Since the PRCs found in the dorsal cirri of *E. complanata* are structurally indistinguishable from typical PRCs present in pigmented eyes, photoreception of these cells is highly probable.

Whereas phaosomes are the only photoreceptor elements present in Clitellata (see Döring et al. 2013), only a few cases of true phaosomes have been described in polychaetes so far (Nørrevang 1974; Verger-Bocquet 1981; Kristensen and Nørrevang 1982; Purschke 1993; Purschke

and Jouin-Toulmond 1993; Hessling and Purschke 2000; Wilkens and Purschke 2009). In polychaetes, these PRCs may either be of the ciliary or rhabdomeric type. Whereas so-called ectopic eyes, i.e., eyes outside the cephalic region, have been found in a number of polychaete species (Purschke et al. 2006; Backfisch et al. 2013), unpigmented PRCs and presence of r-opsin have thus far only been shown to occur in the parapodia of *Platynereis dumerilii* (Backfisch et al. 2013). However, the ultrastructure of these unpigmented PRCs in this species is still unknown. The present example confirms the hypothesis of Backfisch et al. (2013) that non-cephalic PRCs are more widespread than previously assumed and may reflect more ancient aspects of photosensitive systems. Discovery of non-cephalic photoreceptive structures is facilitated by the presence of shading pigment and then already known for many years. However, unpigmented PRCs might be more abundant than currently known, since in ultrastructural analyses they are mainly detected just by chance.

Conclusions

Branchiae and dorsal cirri are rather complex organs in polychaetous Annelida. In *E. complanata*, both appendages are supplied with musculature, blood vessels and nervous tissue. Whereas the branchiae show considerable features indicative for gas exchange such as bands of motile cilia, a thin cuticle and subepithelial as well as intraepidermal blood spaces, the dorsal cirri are primarily sense organs although supplied with a blind-ending blood vessel. In the branchiae, the terminal blood spaces are intraepidermal and are very close to the surface as has been observed in certain other species as well. In addition, the branchiae are equipped with numerous receptor cells which are of one type and assumedly have the same function such as modulation of the ventilation of the branchiae. Given the larger surface area of the branchiae, the total number of receptor cells on the branchiae is similar to that present in the dorsal cirrus, which exhibits a higher density of receptor cells but less space. By contrast, these cirri are probably multimodal sensory structures possessing a variety of receptor cells, the majority of which is regarded to represent mechanoreceptor cells. However, unexpectedly a few unpigmented photoreceptor cells were found in the basal joint of each cirrus. Since these most likely cannot function as eyes or ocelli and thus in avoiding predators, their main function may be providing information whether the respective segments are exposed or buried in the substratum and may be protected or not.

Acknowledgements We are grateful to the head of our department, Prof Dr. A. Paululat, Osnabrueck, for various kinds of support including hospitality of one of us (DW) and discussions. Thanks are also due to K. Etzold and W. Mangerich, Osnabrueck, for various kinds of technical assistance, particularly for introducing MH and LO to electron microscopy techniques. The project was in part funded by the NSERC (DW).

Compliance with ethical standards

Conflict of interest The authors declare that they have no conflict of interest.

Ethical standard We neither used endangered species nor were the investigated animals collected in protected areas; instead the animals stem from a laboratory culture. All applicable international, national and/or institutional guidelines for the care and use of animals were followed.

References

Arendt D, Tessmar-Raible K, Synman H, Dorresteijn A, Wittbrodt J (2004) Ciliary photoreceptors with a vertebrate-type opsin in an invertebrate brain. Science 306:869–871

Arendt D, Hausen H, Purschke G (2009) The 'division of labour' model of eye evolution. Philos Trans R Soc B Biol Sci 364:2809–2817

Backfisch B, Rajan VBV, Fischer RM, Lohs C, Arboleda E, Tessmar-Raible K, Raible F (2013) Stable transgenesis in the marine annelid *Platynereis dumerilii* sheds new light on photoreceptor evolution. Proc Natl Acad Sci USA 110:193–198

Boilly-Marer Y (1972) Étude ultrastructurale des cirres parapodiaux de Nereidiens atoques (Annélides, Polychètes). Z Zellforsch mikrosk Anat 131:309–327

Bullock TH (1965) Annelida. In: Bullock TH, Horridge GA (eds) Structure and function in the nervous systems of invertebrates. Freeman & Co, San Francisco, pp 661–789

Clark RB (1956) The blood vascular system of *Nephtys* (Annelida, Polychaeta). Q J Microsc Sci 97:235–249

Döring C, Gosda J, Tessmar-Raible K, Hausen H, Arendt D, Purschke G (2013) Evolution of clitellate phaosomes from rhabdomeric photoreceptor cells of polychaetes—a study in the leech *Helobdella robusta* (Annelida, Sedentaria, Clitellata). Front Zool 10(52):1–14

Dorsett DA, Hyde R (1969) The fine structure of the compound sense organs on the cirri of *Nereis diversicolor*. Z Zellforsch mikrosk Anat 97:512–527

Eakin RM, Hermans CO (1988) Eyes. In: Westheide W, Hermans CO (eds) The ultrastructure of Polychaeta. Microfauna Marina, vol 4, pp 135–156

Ermak TH, Eakin RM (1976) Fine structure of the cerebral and pygidial ocelli in *Chone ecaudata* (Polychaeta: Sabellidae). J Ultrastruct Res 54:243–260

Fauchald K (1977) The polychaete worms: definitions and keys to the orders, families and genera. Nat Hist Mus Los Angel Cty 28:1–190

Fransen ME (1988) Coelomic and vascular systems. In: Westheide W, Hermans CO (eds) The ultrastructure of Polychaeta. Microfauna Marina, vol 4, pp 199–213

Gardiner SL (1988) Respiratory and feeding appendages. In: Westheide W, Hermans CO (eds) The ultrastructure of Polychaeta. Microfauna Marina ,vol 4, pp 37–43

Gardiner SL (1992) Polychaeta: General organization, integument, musculature, coelom and vascular system. In: Harrison FW, Gardiner SL (eds) Microscopic anatomy of invertebrates. Annelida, vol 7. Wiley-Liss, Chichester, pp 19–52

George JD, Hartmann-Schröder G (1985) Polychaetes: Britisch Amphinomida, Spinterida & Eunicida. In: Kermack DM, Barnes RSK (eds) Synopses of the British Fauna, vol 32. Brill & Backhuys, London, pp 1–221

Hauenschild C, Fischer A (1969) *Platynereis dumerilii*. Mikroskopische Anatomie, Fortpflanzung, Entwicklung. In: Czihak G (ed) Großes Zoologisches Praktikum, vol 10b. Gustav Fischer, Stuttgart, pp 1–55

Hausen H (2005) Comparative structure of the epidermis in polychaetes (Annelida). Hydrobiologia 535(536):25–35

Hessling R, Purschke G (2000) Immunohistochemical (CLSM) and ultrastructural analysis of the central nervous system and sense organs in *Aeolosoma hemprichi* (Annelida, Aeolosomatidae). Zoomorphology 120:65–78

Horridge GA (1963) Proprioceptors, bristle receptors, efferent sensory impulses, neurofibrils and number of axons in the parapodial nerve of the polychaete *Harmothoe*. Proc R Soc Lond B Biol Sci 157:199–222

Huusgaard RS, Vismann B, Kühl M, Macnaugton M, Colmander V, Rouse GW, Glover AG, Dahlgren T, Worsaae K (2012) The potent respiratory system of *Osedax mucofloris* (Siboglinidae, Annelida)—a prerequisite for the origin of bone-eating *Osedax*? Plos ONE 7:e35975

Jouin C, Gaill F (1990) Gills of hydrothermal vent annelids: structure, ultrastructure and functional implications in two alvinellid species. Prog Oceanogr 24:59–69

Jouin C, Toulmond A (1989) The ultrastructure of the gill of the lugworm *Arenicola marina* (L.) (Annelida, Polychaeta). Acta Zool (Stockholm) 70:121–129

Jouin C, Tchernigovtzeff C, Baucher MF, Toulmond A (1985) Fine structure of probable mechano- and chemoreceptors in the caudal epidermis of the lugworm *Arenicola marina* (Annelida, Polychaeta). Zoomorphology 105:76–82

Jouin-Toulmond C, Hourdez S (2006) Morphology, ultrastructure and functional anatomy of the branchial organ of *Terebellides stroemii* (Polychaeta: Trichobranchidae) and remarks on the systematic position of the genus *Terebellides*. Cah Biol Mar 47:287–299

Jouin-Toulmond C, Augustin D, Desbruyères D, Toulmond A (1996) The gas transfer system in alvinellids (Annelida, Polychaeta, Terebellidae). Anatomy and ultrastructure of the anterior circulatory system and characterization of a coelomic, intracellular haemoglobin. Cah Biol Mar 37:135–151

Kristensen RM, Nørrevang A (1982) Description of *Psammodrilus aedificator* sp. n. (Polychaeta), with notes on the Arctic interstitial fauna of Disko Island, W. Greenland. Zool Scr 11:265–279

Lawry JV Jr (1967) Structure and function of the parapodial cirri of the polynoid polychaete, *Harmothoë*. Z Zellforsch mikrosk Anat 82:345–361

Menendez A, Arias JL, Tolivia D, Alvarez-Uria M (1984) Ultrastructure of gill epithelial cells of *Diopatra neapolitana* (Annelida, Polychaeta). Zoomorphology 104:304–309

Nicoll PA (1954) The anatomy and behavior of the vascular system in *Nereis virens* and *Nereis limbata*. Biol Bull 106:69–82

Nørrevang A (1974) Photoreceptors of the phaosome (hirudinean) type in a pogonophore. Zool Anz 193:297–304

O'Donnell MJ (1997) Mechanisms of excretion and ion transport in invertebrates. In: Dantzler WH (ed) Comparative physiology. Oxford University Press, New York, pp 1207–1289

Purschke G (1993) Structure of the prostomial appendages and the central nervous system in the Protodrilida (Polychaeta). Zoomorphology 113:1–20

Purschke G (2003) Ultrastructure of phaosomous photoreceptors in *Stylaria lacustris* (Naididae, "Oligochaeta", Clitellata) and their importance for the position of the Clitellata in the phylogenetic system of the Annelida. J Zool Syst Evolut Res 41:100–108

Purschke G (2005) Sense organs in polychaetes (Annelida). Hydrobiologia 535(536):53–78

Purschke G (2016) Annelida: basal groups and Pleistoannelida. In: Schmidt-Rhaesa A, Harzsch S, Purschke G (eds) Structure and evolution of invertebrate nervous systems. Oxford University Press, Oxford, pp 254–312

Purschke G, Hausen H (2007) Lateral organs in sedentary polychaetes (Annelida)—ultrastructure and phylogenetic significance of an insufficiently known sense organ. Acta Zool (Stockholm) 88:23–39

Purschke G, Jouin-Toulmond C (1993) Ultrastructure of presumed ocelli in *Parenterodrilus taenioides* (Polychaeta, Protodrilidae) and their phylogenetic significance. Acta Zool (Stockholm) 74:247–256

Purschke G, Nowak K (2015) Ultrastructure of pigmented eyes in Dorvilleidae (Annelida, Errantia, Eunicida) and their importance for understanding the evolution of eyes in polychaetes. Acta Zool (Stockholm) 96:67–81

Purschke G, Arendt D, Hausen H, Müller MCM (2006) Photoreceptor cells and eyes in Annelida. Arthropod Struct Dev 35:211–230

Purschke G, Bleidorn C, Struck T (2014) Systematics, evolution and phylogeny of Annelida—a morphological perspective. Mem Mus Vic 71:247–269

Ramirez MD, Speiser DI, Pankey MS, Oakley TH (2011) Understanding the dermal light sense in the context of integrative photoreceptor cell biology. Vis Neurosci 28:265–279

Randel N, Bezares-Calderón LA, Gühmann M, Shahidi R, Jékely G (2013) Expression dynamics and protein localization of rhabdomeric opsins in *Platynereis* larvae. Integr Comp Biol 53:7–16

Rouse GW, Pleijel F (2001) Polychaetes. Oxford University Press, Oxford

Ruppert EE (1991) Introduction to the aschelminth phyla: a consideration of mesoderm, body cavities, and cuticle. In: Harrisson FW, Ruppert EE (eds) Microscopic anatomy of invertebrates. Wiley-Liss, New York, pp 1–17

Schlawny A, Grünig C, Pfannenstiel HD (1991) Sensory and secretory cells of *Ophryotrocha puerilis* (Polychaeta). Zoomorphology 110:209–215

Schmidt-Rhaesa A (2007) The evolution of organ systems. Oxford University Press, Oxford

Shigeno S, Ogura A, Mori T, Toyohara H, Yoshida T, Tsuchida S, Fujikura K (2014) Sensing deep extreme environments: the receptor cell types, brain centers, and multi-layer neural packaging of hydrothermal vent endemic worms. Front Zool 11(82):1–19

Southward EC, Schulze A, Gardiner SL (2005) Pogonophora (Annelida): form and function. Hydrobiologia 535(536):227–251

Storch V, Alberti G (1978) Ultrastructural observations on the gills of polychaetes. Helgol Meeresunter 31:169–179

Storch V, Gaill F (1986) Ultrastructural observations on feeding appendages and gills of *Alvinella pompejana* (Annelida, Polychaeta). Helgol Meeresunter 40:309–319

Storch V, Schlötzer-Schrehardt U (1988) Sensory structures. In: Westheide W, Hermans CO (eds) The ultrastructure of Polychaeta. Microfauna Marina, vol 4, pp 121–133

Struck TH, Paul C, Hill N, Hartmann S, Hoesel C, Kube M, Lieb B, Meyer A, Tiedemann R, Purschke G, Bleidorn C (2011) Phylogenomic analyses unravel annelid evolution. Nature 471:95–98

Struck TH, Golombek A, Weigert A, Franke FA, Westheide W, Purschke G, Bleidorn C, Halanych KM (2015) The evolution of annelids reveals two adaptive routes to the interstitial realm. Curr Biol 25:1993–1999

Suschenko D, Purschke G (2009) Ultrastructure of pigmented adult eyes in errant polychaetes (Annelida): implications for annelid evolution. Zoomorphology 128:75–96

Thiel D, Hugenschütt M, Meyer H, Paululat A, Quijada-Rodriguez AR, Purschke G, Weihrauch D (2016) Ammonia excretion in the marine polychaete *Eurythoe complanata* (Annelida). J Exp Biol. doi:10.1242/jeb.145615

Todt C, Tyler S (2007) Ciliary receptors associated with the mouth and pharynx of Acoela (Acoelomorpha): a comparative ultrastructural study. Acta Zool (Stockholm) 88:41–58

Verger-Bocquet M (1981) Étude comparative, au niveau infrastructural, entre l'oeil de souche et les taches oculaires du stolon chez *Syllis spongicola* (Annélide, Polychète). Arch zool exp gén 122:253–258

Verger-Bocquet M (1992) Polychaeta: sensory structures. In: Harrison FW, Gardiner SL (eds) Microscopic anatomy of invertebrates, vol 7., AnnelidaWiley-Liss, Chichester, pp 181–196

Weigert A, Helm C, Meyer M, Nickel B, Arendt D, Hausdorf B, Santos SR, Halanych KM, Purschke G, Bleidorn C, Struck TH (2014) Illuminating the base of the annelid tree using transcriptomics. Mol Biol Evol 31:1391–1401

Welsch U, Storch V, Richards KS (1984) Epidermal cells. In: Bereiter-Hahn J, Matoltsy AG, Richards KS (eds) Biology of the integument, vol 1., InvertebratesSpringer, Berlin, pp 269–296

Westheide W (1997) The direction of evolution within the Polychaeta. J Nat Hist 31:1–15

Westheide W (2008) Polychaetes: interstitial families. In: Crothers JH, Hayward PJ (eds) Synopses of the British fauna, vol 44, 2nd edn. Field Studies Council, Shrewsbury, pp 1–169

Westheide W, Purschke G (1988) Organism processing. In: Higgins RP, Thiel H (eds) Introduction to the study of meiofauna. Smithsonian Institution Press, Washington, pp 146–160

Wilkens V, Purschke G (2009) Pigmented eyes, photoreceptor-like sense organs and central nervous system in the polychaete *Scoloplos armiger* (Orbiniidae, Annelida) and their phylogenetic importance. J Morphol 270:1–15